MYCOLOGIA

Mycologia

ISSN: 0027-5514 (Print) 1557-2536 (Online) Journal homepage: www.tandfonline.com/journals/umyc20

Molecular systematics of two sister clades, the *Fusarium concolor* and *F. babinda* species complexes, and the discovery of a novel microcycle macroconidium–producing species from South Africa

Adriaana Jacobs-Venter, Imane Laraba, David M. Geiser, Mark Busman, Martha M. Vaughan, Robert H. Proctor, Susan P. McCormick & Kerry O'Donnell

To cite this article: Adriaana Jacobs-Venter, Imane Laraba, David M. Geiser, Mark Busman, Martha M. Vaughan, Robert H. Proctor, Susan P. McCormick & Kerry O'Donnell (2018) Molecular systematics of two sister clades, the *Fusarium concolor* and *F. babinda* species complexes, and the discovery of a novel microcycle macroconidium–producing species from South Africa, Mycologia, 110:6, 1189-1204, DOI: 10.1080/00275514.2018.1526619

To link to this article: https://doi.org/10.1080/00275514.2018.1526619

MYCOLOGIA
2018, VOL. 110, NO. 6, 1189–1204
https://doi.org/10.1080/00275514.2018.1526619

Taylor & Francis
Taylor & Francis Group

Molecular systematics of two sister clades, the *Fusarium concolor* and *F. babinda* species complexes, and the discovery of a novel microcycle macroconidium–producing species from South Africa

Adriaana Jacobs-Venter[a], Imane Laraba [b], David M. Geiser[c], Mark Busman [d], Martha M. Vaughan[d], Robert H. Proctor [d], Susan P. McCormick [d], and Kerry O'Donnell [d]

[a]Biosystematics Unit, Plant Health and Protection, Agricultural Research Council, Pretoria, 0001 South Africa; [b]Laboratoire de phytopathologie et de biologie moléculaire, département de botanique, Ecole Nationale Supérieure Agronomique, Algiers, Algeria; [c]Department of Plant Pathology and Environmental Microbiology, Pennsylvania State University, University Park, Pennsylvania 16802; [d]Mycotoxin Prevention and Applied Microbiology Research Unit, National Center for Agricultural Utilization Research, Agricultural Research Service, US Department of Agriculture, Peoria, Illinois 60604-3999

ABSTRACT

Multilocus DNA sequence data were used to investigate species identity and diversity in two sister clades, the *Fusarium concolor* (FCOSC) and *F. babinda* species complexes. Of the 109 isolates analyzed, only 4 were received correctly identified to species and these included 1/46 *F. concolor*, 1/31 *F. babinda*, and 2/3 *F. anguioides*. The majority of the *F. concolor* and *F. babinda* isolates were received as *F. polyphialidicum*, which is a heterotypic synonym of the former species. Previously documented from South America, Africa, Europe, and Australia, our data show that *F. concolor* is also present in North America. The present study expands the known distribution of *F. babinda* in Australia to Asia, Europe, and North America. The molecular phylogenetic results support the recognition of a novel *Fusarium* species within the FCOSC, which is described and illustrated here as *F. austroafricanum*, sp. nov. It was isolated as an endophyte of kikuyu grass associated with a putative mycotoxicosis of cattle and from plant debris in soil in South Africa. *Fusarium austroafricanum* is most similar morphologically to *F. concolor* and *F. babinda* but differs from the latter two species in producing (i) much longer macroconidia in which the apical cell is blunt to slightly papillate and the basal cell is only slightly notched and (ii) macroconidia via microcycle conidiation on water agar. BLASTn searches of the whole genome sequence of *F. austroafricanum* NRRL 53441 were conducted to predict mycotoxin potential, using genes known to be essential for the synthesis of several mycotoxins and biologically active metabolites. Based on the presence of intact gene clusters that confer the ability to synthesize mycotoxins and pigments, we analyzed cracked corn kernel cultures of *F. austroafricanum* via liquid chromatography–mass spectrometry (LC-MS) but failed to detect these metabolites in vitro.

ARTICLE HISTORY
Received 6 June 2018
Accepted 18 September 2018

KEYWORDS
Fusarium austroafricanum; *Fusarium babinda*; *Fusarium polyphialidicum*; gene genealogies; morphology; mycotoxins; pathogenicity; phylogenetic species recognition; 1 new taxon

INTRODUCTION

Fusarium's rank as one of the world's most important genera of mycotoxigenic phytopathogens helps explain why it has been the subject of intensive molecular phylogenetic study over the past two decades (reviewed in Aoki et al. 2014). These studies indicate that the genus comprises over 300 phylogenetically distinct species distributed among 23 clades referred to as species complexes (Laurence et al. 2011; O'Donnell et al. 2013; Zhou et al. 2016; Sandoval-Denis et al. 2018). Multilocus molecular phylogenetic analyses over the past 20 y have contributed significantly to the discovery and formal description of over 100 genealogically exclusive species; however, many phylospecies remain unnamed in species-rich groups such as the *F. solani* and *F. incarnatum-equiseti* species complexes (O'Donnell et al. 2008, 2009). The most intensive molecular systematic studies to date have focused on resolving evolutionary relationships and formally describing species within clades that contain economically important mycotoxin-producing plant pathogens such as the *F. fujikuroi* (Nirenberg and O'Donnell 1998; O'Donnell et al. 1998; Herron et al. 2015; Sandoval-Denis et al. 2018) and *F. sambucinum* (Gräfenhan et al. 2016 and references therein) species complexes as defined in O'Donnell et al. (2013).

CONTACT Kerry O'Donnell kerry.odonnell@ars.usda.gov
Supplemental data for this article can be accessed on the publisher's Web site.

Published online 06 Dec 2018

The *Fusarium concolor* and *F. babinda* species complexes comprise two sister clades (Kim et al. 2017) whose origin dates to the mid-Oligocene, approximately 28 million years ago (Mya) (O'Donnell et al. 2013). While conducting BLASTn queries of National Center for Biotechnology Information (NCBI) GenBank (https://www.ncbi.nlm.nih.gov/) and *Fusarium MLST* (http://www.westerdijkinstitute.nl/fusarium/), using a partial translation elongation factor 1-α (*TEF1*) sequence of the ex-type strain of *F. concolor* CBS 183.34 as the query, Balmas et al. (2010) serendipitously discovered that this species appears to be conspecific with *F. polyphialidicum* CBS 961.87. The original description of *F. concolor* was based on a single isolate recovered from the base of a diseased barley plant collected near Montevideo, Uruguay (Reinking 1934), whereas *F. polyphialidicum* was isolated initially from plant debris in soil from several provinces in South Africa (Marasas et al. 1986). Following the formal description of the latter species, it was reported from numerous sources, including gypsy moth larvae in eastern North America (Hajek et al. 1993, 1997), soils and mouldy sorghum in Australia (Gott et al. 1994), *Pinus strobus* seed in Wisconsin (Ocamb et al. 2002), and a human corneal ulcer in Spain (Guarro et al. 2003) (TABLE 1). *Fusarium anguioides* Sherb. is the only other described species in the *F. concolor* clade (O'Donnell et al. 2013). It was first isolated and described from rotten potato tubers (Sherbakoff 1915) and subsequently neotypified based on isolates from soil in a bamboo grove in China (Nelson et al. 1995). Isolates of *F. babinda*, the only described species within a species complex by the same name, were recovered from plant debris in soils from wet sclerophyll and rain forests in eastern Australia (Summerell et al. 1995).

Given the significant limitations of morphological species recognition, and the lack of data concerning their mycotoxin potential (Munkvold 2017) and pathogenicity to wheat, we initiated the present study to (i) determine the identity of isolates received as and accessioned in the ARS Culture Collection (NRRL) as *F. anguioides, F. babinda, F. concolor, F. polyphialidicum*, and phylogenetically related fusaria received as *Fusarium* sp.; (ii) formally describe a novel species in the *Fusarium concolor* species complex (FCOSC) from kikuyu grass and plant debris in soil from South Africa; (iii) evaluate their mycotoxin potential by in silico whole genome sequence analyses and liquid chromatographic–mass spectrometric (LC-MS) analyses of cracked maize kernel cultures; (iv) assess whether these fusaria can induce head blight of wheat; and (v) conduct a polymerase chain reaction (PCR) screen for *MAT* idiomorph to predict their sexual reproductive mode.

MATERIALS AND METHODS

Fungal isolates studied.—The 109 *Fusarium* isolates included in the present study were recovered during pathogen surveys or obtained as pure cultures from publically accessible culture collections (TABLE 1). All of the strains were accessioned in the ARS Culture Collection (NRRL) where they are available for distribution upon request (https://nrrl.ncaur.usda.gov/). Pure cultures of fusaria isolated from kikuyu grass and plant debris from South Africa were obtained by surface disinfecting ~4-mm pieces of plant material with 2% sodium hypochlorite for 5 min. Afterwards the specimens were rinsed twice with sterile water, blotted dry, and then plated onto *Fusarium*-selective medium containing 20 g agar, 15 g peptone, 1 g KH_2PO_4, 0.5 g $MgSO_4{\cdot}7H_2O$, 1 g pentachloronitrobenzene (P8556; Millipore-Sigma, St. Louis, Missouri), and 4 mL penicillin-streptomycin-neomycin solution (P4083; MilliporeSigma) in 1 L water. Single-spore cultures were established by isolating germinating conidia on 3% water agar.

Molecular phylogenetics.—Methods for culturing isolates to obtain mycelium for extracting genomic DNA and primers used for polymerase chain amplification (PCR) of portions of three phylogenetically informative genes (translation elongation factor 1-α [*TEF1*] and DNA-directed RNA polymerase II largest subunit [*RPB1*] and second largest subunit [*RPB2*]) and Sanger sequencing were published previously (see table 2 in O'Donnell et al. 2010). After sequence chromatograms were obtained with an ABI 3730 genetic analyzer (ABI, Emeryville, California), they were edited using Sequencher 5.2.4 (Gene Codes Corp., Ann Arbor, Michigan) and then exported as NEXUS files. DNA sequences in the NEXUS file were aligned using the MUSCLE algorithm (Edgar 2004) and then improved manually using TextPad 5.1.0 for Windows (http://www.textpad.com/). GARLI 2.01 (Zwickl 2006) was used to conduct 1000 maximum likelihood (ML) bootstrap pseudoreplicates on the CIPRES Science Gateway TeraGrid (https://www.phylo.org/) employing the GTR+I+Γ model of molecular evolution. PAUP* 4.0b10 (Swofford 2003) was used to conduct maximum parsimony (MP) analyses of the individual partitions and combined data set, using the heuristic search option with 1000 random sequence addition replicates, MULPARS on, and tree bisection-reconnection branch swapping. Clade support was assessed by 1000 bootstrap pseudoreplicates of the data. Comparison of MP bootstrap support in the individual partitions did not identify any conflict between strongly supported nodes, so they were analyzed as

Table 1. Strain histories.

Species ID[a]	NRRL no.[b]	Equivalent no.[c]	Received as	Host/substrate	Geographic origin	MAT[d]
F. anguioides	31043	FRC R-7361	*F. anguioides*	Bamboo	China	1
F. anguioides [NT]	25385	ATCC 66485	*F. anguioides*	Bamboo	China	1
F. austroafricanum	53441	FRC M-2406 = PPRI 23546	*F. polyphialidicum*	Plant debris in soil	Mpumalanga, South Africa	1
F. austroafricanum	66742	PPRI 10412	*F. redolens*	Kikuyu grass	Humansdorp, South Africa	1
F. austroafricanum [T]	66741	PPRI 23548	*F. redolens*	Kikuyu grass	Humansdorp, South Africa	1
F. babinda	25105	ARSEF 3532	*Fusarium* sp.	*Lymantria dispar* [Lepidoptera]	USA, Maryland	2
F. babinda	25529	ARSEF 3692	*F. polyphialidicum*	*Lymantria dispar* [Lepidoptera]	USA, New York	1
F. babinda	25530	ARSEF 3693	*F. polyphialidicum*	*Lymantria dispar* [Lepidoptera]	USA, New York	1
F. babinda	25531	ARSEF 3694	*F. polyphialidicum*	*Lymantria dispar* [Lepidoptera]	USA, Massachusetts	1
F. babinda	25532	ARSEF 3695	*F. polyphialidicum*	*Lymantria dispar* [Lepidoptera]	USA, Virginia	1
F. babinda	25533	ARSEF 3696	*F. polyphialidicum*	*Lymantria dispar* [Lepidoptera]	USA, Maryland	1
F. babinda	25539	F11165 = CBS 396.96	*F. babinda*	Rainforest soil	Queensland, Australia	1
F. babinda	26207	Ocamb USF 357	*F. polyphialidicum*	White pine seed	USA, Minnesota	1
F. babinda	26208	Ocamb USF 367	*F. polyphialidicum*	White pine seed	USA, Minnesota	1
F. babinda	26209	Ocamb USF 363	*F. polyphialidicum*	White pine seed	USA, Minnesota	1
F. babinda	52755	ARSEF 3483	*Fusarium* sp.	*Lymantria dispar* [Lepidoptera]	USA, Virginia	2
F. babinda	52759	ARSEF 3916	*F. polyphialidicum*	*Lymantria dispar* [Lepidoptera]	USA, Pennsylvania	2
F. babinda	52779	ARSEF 5803	*Fusarium* sp.	*Adelges tsugae* [Hemiptera]	USA, Massachusetts	1
F. babinda	52780	ARSEF 5825	*Fusarium* sp.	*Adelges tsugae* [Hemiptera]	USA, Massachusetts	1
F. babinda	53466	FRC R-7430	*F. polyphialidicum*	Tea bush soil	China	1
F. babinda	53467	FRC R-7431	*F. polyphialidicum*	Tea bush soil	China	2
F. babinda	53468	FRC R-7433	*F. polyphialidicum*	Tea bush soil	China	2
F. babinda	53469	FRC R-7434	*F. polyphialidicum*	Tea bush soil	China	1
F. babinda	53470	FRC R-7436	*F. polyphialidicum*	Tea bush soil	China	2
F. babinda	53471	FRC R-7442	*F. polyphialidicum*	Tea bush soil	China	1
F. babinda	53472	FRC R-7443	*F. polyphialidicum*	Tea bush soil	China	1
F. babinda	53487	FRC R-9169	*F. polyphialidicum*	Douglas fir	USA, Pennsylvania	1
F. babinda	53488	FRC R-9251	*F. polyphialidicum*	Douglas fir	USA, Pennsylvania	1
F. babinda	53489	FRC R-9252	*F. polyphialidicum*	Douglas fir seed	Canada	1
F. babinda	53497	FRC R-9399	*F. polyphialidicum*	*Lymantria dispar* [Lepidoptera]	USA, Pennsylvania	2
F. babinda	53498	FRC R-9409	*F. polyphialidicum*	honey locust	USA, Minnesota	2
F. babinda	53500	FRC R-9446	*F. polyphialidicum*	White pine seed	USA, Minnesota	1
F. babinda	53501	FRC R-9449	*F. polyphialidicum*	White pine seed	USA, Minnesota	1
F. babinda	53502	FRC R-9450	*F. polyphialidicum*	White pine seed	USA, Minnesota	1
F. babinda	53504	FRC R-9493	*F. polyphialidicum*	Conifer seed	USA, Minnesota	2
F. babinda	53505	FRC R-10061	*F. polyphialidicum*	Unknown	USA, Mississippi	1
F. concolor	13459	CBS 961.87	*F. polyphialidicum* [T]	Plant debris in soil	South Africa	2
F. concolor [T]	13994	CBS 183.34	*F. concolor*	Barley	Uruguay	1
F. concolor	26423	CBS 676.94	*F. polyphialidicum*	Soil	South Africa	2
F. concolor	36205	CBS 111770	*F. polyphialidicum*	Human eye	Spain	1
F. concolor	44907	Balmas 24-A6	*Fusarium* sp.	Soil	Sardinia-Italy	1
F. concolor	44908	Balmas 24-A7	*Fusarium* sp.	Soil	Sardinia-Italy	1
F. concolor	44912	Balmas 24-B4	*Fusarium* sp.	Soil	Sardinia-Italy	1
F. concolor	44915	Balmas 24-B15	*Fusarium* sp.	Soil	Sardinia-Italy	1
F. concolor	44918	Balmas 24-B32	*Fusarium* sp.	Soil	Sardinia-Italy	2
F. concolor	44919	Balmas 24-B35	*Fusarium* sp.	Soil	Sardinia-Italy	2
F. concolor	44921	Balmas 24-C9	*Fusarium* sp.	Soil	Sardinia-Italy	1
F. concolor	44922	Balmas 24-C14	*Fusarium* sp.	Soil	Sardinia-Italy	1
F. concolor	44927	Balmas 24-EC10	*Fusarium* sp.	Soil	Sardinia-Italy	1
F. concolor	44928	Balmas 24-EC22	*Fusarium* sp.	Soil	Sardinia-Italy	1
F. concolor	52927	ARSEF 3042	*Fusarium* sp.	Nematode [Nemata: Secernentea]	USA, Hawaii	1
F. concolor	53443	FRC M-2413 = DAOM 192992	*F. polyphialidicum*	Vegetation natural	South Africa	1
F. concolor	53444	FRC M-2414 = DAOM 192993	*F. polyphialidicum*	Wheat field soil	South Africa	1
F. concolor	53445	FRC M-2416 = MRC 3568	*F. polyphialidicum*	Wheat field soil	South Africa	1
F. concolor	53446	FRC M-2418 = MRC 3570	*F. polyphialidicum*	Maize	South Africa	1
F. concolor	53447	FRC M-2419 = MRC 3571	*F. polyphialidicum*	Wheat field soil	South Africa	1
F. concolor	53448	FRC M-2425 = DAOM 192994	*F. polyphialidicum*	Wheat field soil	South Africa	1
F. concolor	53449	FRC M-2427 = DAOM 192995	*F. polyphialidicum*	Lucerne soil	South Africa	1
F. concolor	53450	FRC M-2431 = MRC 3678	*F. polyphialidicum*	Lucerne soil	South Africa	1
F. concolor	53451	FRC M-2433 = MRC 3680	*F. polyphialidicum*	Wheat field soil	South Africa	1
F. concolor	53452	FRC M-2435 = CBS 677.94	*F. polyphialidicum*	Maize	South Africa	1
F. concolor	53453	FRC M-2436 = MRC 3691	*F. polyphialidicum*	Maize	South Africa	1
F. concolor	53454	FRC M-2437 = MRC 3698	*F. polyphialidicum*	Vegetation	South Africa	1
F. concolor	53455	FRC M-3251	*F. polyphialidicum*	Soil	South Africa	2
F. concolor	53458	FRC M-3263	*F. polyphialidicum*	Debris from soil	South Africa	1
F. concolor	53459	FRC M-3282	*F. polyphialidicum*	Debris from soil	South Africa	1
F. concolor	53473	FRC R-8339	*F. polyphialidicum*	Debris from soil	South Africa	1
F. concolor	53476	FRC R-8423	*F. polyphialidicum*	Wheat root	USA, Georgia	1
F. concolor	53477	FRC R-8436	*F. polyphialidicum*	Debris from soil	South Africa	1

(*Continued*)

Table 1. (Continued).

Species ID[a]	NRRL no.[b]	Equivalent no.[c]	Received as	Host/substrate	Geographic origin	MAT[d]
F. concolor	53478	FRC R-8437	*F. polyphialidicum*	Debris from soil	South Africa	1
F. concolor	53479	FRC R-8801	*F. polyphialidicum*	Debris from millet soil	Zimbabwe	2
F. concolor	53480	FRC R-8803	*F. polyphialidicum*	Debris from millet soil	Zimbabwe	2
F. concolor	53482	FRC R-8853	*F. polyphialidicum*	Soil sorghum	Zimbabwe	1
F. concolor	53485	FRC R-9064	*F. polyphialidicum*	Debris from millet soil	Zimbabwe	1
F. concolor	53486	FRC R-9065	*F. polyphialidicum*	Debris from millet soil	Zimbabwe	1
F. concolor	53490	FRC R-9364 = F11046	*F. polyphialidicum*	Soil	Australia	2
F. concolor	53491	FRC R-9365 = F11047	*F. polyphialidicum*	Soil	Australia	2
F. concolor	53492	FRC R-9366 = F11045	*F. polyphialidicum*	Soil	Australia	2
F. concolor	53493	FRC R-9373	*F. polyphialidicum*	Winter wheat	Australia	1
F. concolor	53494	FRC R-9374 = F11079	*F. polyphialidicum*	Soil	Australia	1
F. concolor	53495	FRC R-9375 = F11091	*F. polyphialidicum*	Soil	Australia	2
F. concolor	53496	FRC R-9377 = F11093	*F. polyphialidicum*	Soil	Australia	1
F. avenaceum	13955	CBS 172.32	*F. anguioides*	Garden pea	Japan	—
F. subglutinans	53503	FRC R-9492	*F. polyphialidicum*	Conifer seed	USA, Minnesota	—
F. torulosum	28165	DAOM 144596	*F. concolor*	*Picea* sp. seedling	Canada	—
F. verticillioides	53465	FRC M-3362	*F. polyphialidicum*	Debris	South Africa	—
Fusarium sp. FCSC-?	25483	CBS 217.78 = BBA 63778	*F. concolor*	*Pennisetum typhoideum*	Namibia	—
Fusarium sp. FCSC-2	53442	FRC M-2411 = DAOM 192991	*F. polyphialidicum*	Turf between mangos	South Africa	—
Fusarium sp.-1 FFSC	53440	FRC M-2381	*F. polyphialidicum*	Wheat field soil	Zambia	—
Fusarium sp.-2 FFSC	53456	FRC M-3254	*F. polyphialidicum*	Debris from soil	South Africa	—
Fusarium sp.-2 FFSC	53457	FRC M-3255	*F. polyphialidicum*	Debris from soil	South Africa	—
Fusarium sp.-2 FFSC	53460	FRC M-3309	*F. polyphialidicum*	Soil	South Africa	—
Fusarium sp.-2 FFSC	53461	FRC M-3317	*F. polyphialidicum*	Soil	South Africa	—
Fusarium sp.-3 FFSC	53462	FRC M-3321	*F. polyphialidicum*	Debris	South Africa	—
Fusarium sp.-4 FFSC	53463	FRC M-3354	*F. polyphialidicum*	Soil	South Africa	—
Fusarium sp.-5 FFSC	53464	FRC M-3359	*F. polyphialidicum*	Soil	South Africa	—
Fusarium sp. FIESC 2	20491	MUCL 797	*F. concolor*	*Gossypium hirsutum*	Zaire	—
Fusarium sp. FIESC 10	39638	ICMP 5225	*F. concolor*	Unknown	New Zealand	—
Fusarium sp. FIESC 10	39734	ICMP 5644	*F. concolor*	Pasture soil	New Zealand	—
Fusarium sp. FIESC 14	39632	ICMP 5235	*F. concolor*	Garden pea	New Zealand	—
Fusarium sp. FIESC 26	25526	QM 9398	*F. concolor*	Rubiaceae leaf	Java	—
Fusarium sp. FIESC 28	53481	FRC R-8847	*F. polyphialidicum*	Moldy sorghum	Australia	—
Fusarium sp. FIESC 28	53483	FRC R-8899 = F7757	*F. polyphialidicum*	Unknown	Australia	—
Fusarium sp. FIESC 28	53484	FRC R-8902 = F7767	*F. polyphialidicum*	Unknown	Australia	—
Fusarium sp. FIESC ?	28166	DAOM 170309	*F. concolor*	Soil	India	—
Fusarium sp. FLSC	25490	CBS 256.93	*F. polyphialidicum*	*Macadamia temifolia* leaf	Cuba	—
Fusarium sp. FSAMSC	39651	ICMP 5213	*F. concolor*	Squash	New Zealand	—
Fusarium sp. FOSC	25487	CBS 463.91	*F. polyphialidicum*	Human nail	Germany	—
Fusarium sp. FOSC	53499	FRC R-9412	*F. polyphialidicum*	White pine seed	Canada	—

[a]FCSC = *Fusarium chlamydosporum* species complex; FFSC = *F. fujikuroi* species complex; FIESC = *F. incarnatum-equiseti* species complex; FLSC = *F. lateritium* species complex; FOSC = *F. oxysporum* species complex; FSAMSC = *F. sambucinum* species complex; NT = ex-neotype; T = ex-holotype.
[b]NRRL, ARS Culture Collection, Peoria, Illinois.
[c]ARSEF, ARS Collection of Entomopathogenic Fungal Cultures, Ithaca, New York; ATCC, American Type Culture Collection, Manassas, Virginia; Balmas, See Mycologia 102:803-812(2010); BBA, Biologische Bundesanstalt für Land- und Forstwirtschaft, Institute für Mikrobiologie, Berlin, Germany; CBS, Westerdijk Fungal Biodiversity Institute, Utrecht, the Netherlands; DAOM, Biodiversity, Agriculture & Agri-Food Canada, Ottawa, Canada; F, Fusarium Research Laboratory, University of Sydney, Sydney, Australia; FRC, Fusarium Research Center, The Pennsylvania State University, State College, Pennsylvania; ICMP, The International Collection of Microorganisms from Plants, Landcare Research, Auckland, New Zealand; MRC, South African Agricultural Research Council, South Africa; MUCL, Mycotheque de l'Universite catholique de Louvain, Louvain-la-Neuve, Belgium; Ocamb, C. Ocamb, Oregon State University, Corvallis, Oregon; PPRI, Plant Protection Research, Agricultural Research Council, Pretoria, South Africa; QM, Quatermaster Culture Collection housed in NRRL, Peoria, Illinois.
[d]1, MAT1-1; 2, MAT1-2; –, not tested.

a combined data set. The NEXUS file and one of the most-parsimonious trees inferred from the combined data set were deposited in TreeBASE as study numbers S23166 and Tr113232, respectively; DNA sequences were deposited in GenBank under accession numbers MH742492–MH742713.

Determination of mating type idiomorph and secondary metabolite biosynthetic potential.— Strains were screened for *MAT1-1* and *MAT1-2* idiomorphs using a published PCR assay (Kerényi et al. 2004; TABLE 1). This assay yielded positive genotypes for all of the strains except for those of *F. anguioides*.

Table 2. Summary of maximum parsimony phylogenetic analyses.

Locus	Alignment length (bp)	Number of MPTs	MPT length	CI	RI	Syn	Aut	Bootstrap support (%) *F. austroafricanum*
TEF1	714	28	134	0.96	1.0	111	6	100
RPB1	1859	>1000	311	0.94	1.0	266	3	98
RPB2	1797	44	277	0.91	0.99	233	2	100
Combined	4370	>50 000	728	0.93	0.99	610	11	100

Note. CI = consistency index; MPTs = most-parsimonous trees; RI = retention index; Aut = autapomorphy = uniquely derived character or parsimony uninformative character; Syn = synapomorphy or parsimony-informative character.

Therefore, whole genome sequence data of *Fusarium anguioides* NRRL 25385, *F. austroafricanum* NRRL 66741, *F. babinda* NRRL 25539, and *F. concolor* NRRL 13994 were obtained using an Illumina MiSeq instrument with the of aim using it to design a PCR assay for typing *MAT* in *F. anguioides*. After the sequence reads were trimmed and assembled using applications in CLC Genomics Workbench (CLC bio, Qiagen, Aarhus, Denmark), the BLASTn application in CLC Genomics Workbench was used to search the assembled genomes for the Kerényi et al. (2004) *MAT1-1* and *MAT1-2* primer binding regions. The degenerate Kerényi et al. (2004) forward primers for *MAT1-1* (fusALPHAfor 5′ CGCCCTCT**K**AA**Y**G**S**CTTCATG) and *MAT1-2* (fusHMGfor 5′ CGACCTCCCAA**Y**GC**Y**TACAT) in this assay were replaced, respectively, with the nondegenerated primers MAT111f 5′ CGCCCTCTCAACGCCTTCATG and MAT121f 5′ CGACCTCCCAACGCCTACAT. However, because the reverse primers used by Kerényi et al. (2004) could not be redesigned to work on *F. anguioides*, fusALPHArev and fusHMGrev were replaced with MAT111r 5′ ACAG**H**GTCGCCAGT**R**GTAG and MAT121r 5′ TAGTCAGG**R**TACTGTCGAC, respectively. When the two new primer pairs were used in a PCR assay for *MAT* idiomorph, which was conducted at an annealing temperature of 55 C for 40 cycles, the *MAT1-1* and *MAT1-2* primers amplified fragments 497 and 197 bp in length, respectively. The whole genomes were also screened for the presence and absence of gene clusters that confer the ability to synthesize multiple *Fusarium* mycotoxins and pigments (Edwards et al. 2016; Gräfenhan et al. 2016). Whole genome sequences were deposited in GenBank under BioProject PRJNA485357.

Isolates of the species studied were cultured on V8 juice agar (20% V8 juice, 0.3% $CaCO_3$, 2% agar; Stevens 1974) to obtain conidia that were inoculated on cracked corn kernel cultures (50 g cracked corn + 22 mL water) as previously described (Aoki et al. 2015; Laraba et al. 2018). After the cultures were incubated in the dark for 28 d, 10 g of each solid culture was extracted with 50 mL of acetonitrile:water (1:1, *v*/*v*). The extracts were purified using 13-mm 0.45-µm nylon Acrodisc syringe filters (Millipore-Sigma, St. Louis, Missouri) and then analyzed by high-performance liquid chromatography–mass spectrometry (HPLC-MS) using a Dionex model U3000 liquid chromatography system (Thermo Scientific, Waltham, Massachusetts) and a QTRAP 3200 mass spectrometer (AB SCIEX; Concord, Ontario, Canada). To observe a wide range of metabolites, the LC-MS analyses were conducted with the full scan in positive ionization mode. In addition, positive-mode tandem mass spectrometry was used to assay for production of bikaverin (Busman et al. 2012), 2-amino-14,16-dimethyloctadecan-3-ol (2-AOD-ol; Uhlig 2005), and fusaric acid (Brown et al. 2015); analyses were also conducted in negative-mode ionization to detect moniliformin mycotoxin.

Pathogenicity on spring wheat and mycotoxin quantification from wheat spikelets.—To assess whether isolates of *Fusarium anguioides* (NRRL 25385), *F. austroafricanum* (NRRL 53441, 53489, and 66741), *F. babinda* (NRRL 53497), and *F. concolor* (NRRL 13459 and 13994) could cause head blight on wheat, the susceptible spring wheat cultivar Norm was grown to anthesis in a contained growth room environmentally controlled at 23 C day/20 C night, 500 µmol m^{-2} s^{-1} photosynthetic photo flux density 14-h photoperiod, and 40–50% relative humidity. Flowering wheat heads were inoculated by injecting 10 µL of a 0.04% Tween 20 (Fisher Scientific, Waltham, Massachusetts) suspension containing approximately 10^5 conidia/mL in a single central spikelet. Negative-control heads were injected with sterile 0.04% Tween 20 solution, and positive-control heads were injected with *F. graminearum* NRRL 29169 (= Gz3639 = CBS 110271), a known head blight pathogen. The inoculum concentrations were standardized by counting the number of conidia in the suspension using a hemocytometer. Ten heads were inoculated for each of the treatments (*Fusarium* strains or sterile Tween). Following inoculation, the heads were covered with plastic bags for 3 d to ensure high humidity and foster the initial phase of pathogenesis. Isolates that caused premature

whitening or necrosis of the inoculated spikelet were scored as pathogenic. However, only isolates that were capable of overcoming the plant's defenses and spread to neighboring spikelets were considered aggressive. Symptoms were evaluated throughout a time course of 21 d post inoculation. Since most of the isolates did not spread beyond the point of inoculation, the inoculated spikelet's from two independent heads were combined, frozen in liquid nitrogen, and then freeze-dried overnight. The dried tissue was then ground into a fine powder, and mycotoxins were extracted from approximately 400 mg using 2 mL of acetonitrile:water (86:14, *v*/*v*) for 1 h while shaking. Samples inoculated with *F. graminearum* NRRL 29169 (= Gz3639 = CBS 110271) were analyzed for production of deoxynivalenol (DON) using gas chromatography–mass spectroscopy (GC-MS) as previously described (Aoki et al. 2014). The remaining samples were subjected to LC-MS analysis and tandem mass spectrometry as described above.

Morphological characterization.—Detailed phenotypic data were obtained by culturing isolates in the dark or under an alternating 12 h dark/12 h near-UV black fluorescent and white light cycle in a temperature-controlled incubator (IntellusUltra C8; Percival Scientific, Perry, Iowa) set at 25 C. Isolates were cultured on potato dextrose agar (PDA) in 90-mm Petri plates to characterize colony color using a color atlas (Kornerup and Wanscher 1978). Optimal temperature for growth was determined by placing a 3-mm agar plug taken from a culture grown on PDA and placing it in the center of a 90-mm PDA plate. These were incubated in the dark at six different temperatures at 5 C intervals between 15 and 40 C. Radial growth over 5 d was measured on each plate using four technical replicates to calculate the average daily growth rate. Conidial features were analyzed by culturing isolates on synthetic low-nutrient agar (SNA; Nirenberg 1976) and 2% water agar with four 1 × 1 cm pieces of filter paper placed on the agar surface, and on carnation leaf agar (CLA; Fisher et al. 1982). Isolates were grown on soil extract agar (SEA) to determine whether they could produce chlamydospores and sclerotial bodies (Klotz et al. 1988). Fifty macro- and microconidia, based on the number of septa, 50 chlamydospores, and 30 phialides were measured to determine their dimensions. A Jenopitk ProgRes CCD camera (Jenopitk, Jena, Germany), with Capture Pro 2.8.8 software, was used to record light micrographs obtained with a Zeiss Axioplan microscope (Carl Zeiss, Jena, Germany) fitted with a 40× Plan-neoflur 40×/0.75 objective and differential interference contrast (DIC) optics. Samples for scanning electron microscopy (SEM) were prepared by fixing agar squares approx. 5 × 5 mm in diam for 24–48 h in the dark with 2% aqueous OsO_4 vapors, after which they were dehydrated in a graded ethanol series with 1 h at each step (i.e., 25% 50%, 75%, 95%, 100%). The dehydrated samples were dried using a Samdri-PVT-3D critical point dryer (Tousimis, Rockville, Maryland), using CO_2 as the carrier gas, and then coated with gold in a SPI-Module sputter coater (Structure Probe, West Chester, Pennsylvania) prior to viewing in a JEOL JSM-6400 SEM (Tokyo, Japan).

RESULTS

Molecular phylogenetics.—Portions of *RPB1* (1859 bp alignment, 549 parsimony-informative characters [PICs]), *RPB2* (1779 bp alignment, 510 PICs), and *TEF1* (765 bp alignment, 278 PICs) were analyzed separately to place the 109 strains in species complexes and species (SUPPLEMENTARY FIGS. 1–3). Results of these preliminary analyses indicated that 105/109 strains were received misidentified. The molecular phylogenetic analyses together with BLASTn queries of GenBank indicated that 49 of the 52 isolates in the FCOSC (i.e., 1/3 *F. anguioides*, 3/3 *Fusarium* sp., 45/46 *F. concolor*) and 30/31 *F. babinda* were received misidentified (TABLE 1). In addition, 26 strains accessioned in the ARS Culture Collection (NRRL) as *F. polyphialidicum* (N = 17) or *F. concolor* (N = 9), and one accessioned as *F. anguioides* (NRRL 13955 = CBS 172.32), were identified molecularly as 20 other phylogenetically distinct species from seven different species complexes (TABLE 1).

Based on the preliminary analyses, a three-locus, 81-isolate data set was constructed that included 4370 bp of aligned sequences of 51 strains representing the three species in the FCOSC together with 30 strains of *F. babinda*, which were used to root the phylogeny based on more inclusive analyses (FIG. 1; Kim et al. 2017). Maximum parsimony (MP) and maximum likelihood (ML) bootstrapping (BS) resolved *F. anguioides* as the earliest diverging species lineage in the FCOSC (FIG. 1); this species was also resolved as the reciprocally monophyletic sister of a genealogically exclusive lineage comprising *F. concolor* and a newly discovered species from South Africa described herein as *F. austroafricanum*. MP bootstrap analyses of the individual and combined data sets strongly supported *F. austroafricanum* as a phylogenetically distinct species (TABLE 2). Although isolates of this species were recovered approximately 1400 km apart in South Africa as endophytes of kikuyu grass in the Eastern Cape Province and plant debris in soil in Mpumalanga Province, they shared the same three-locus haplotype. The two isolates

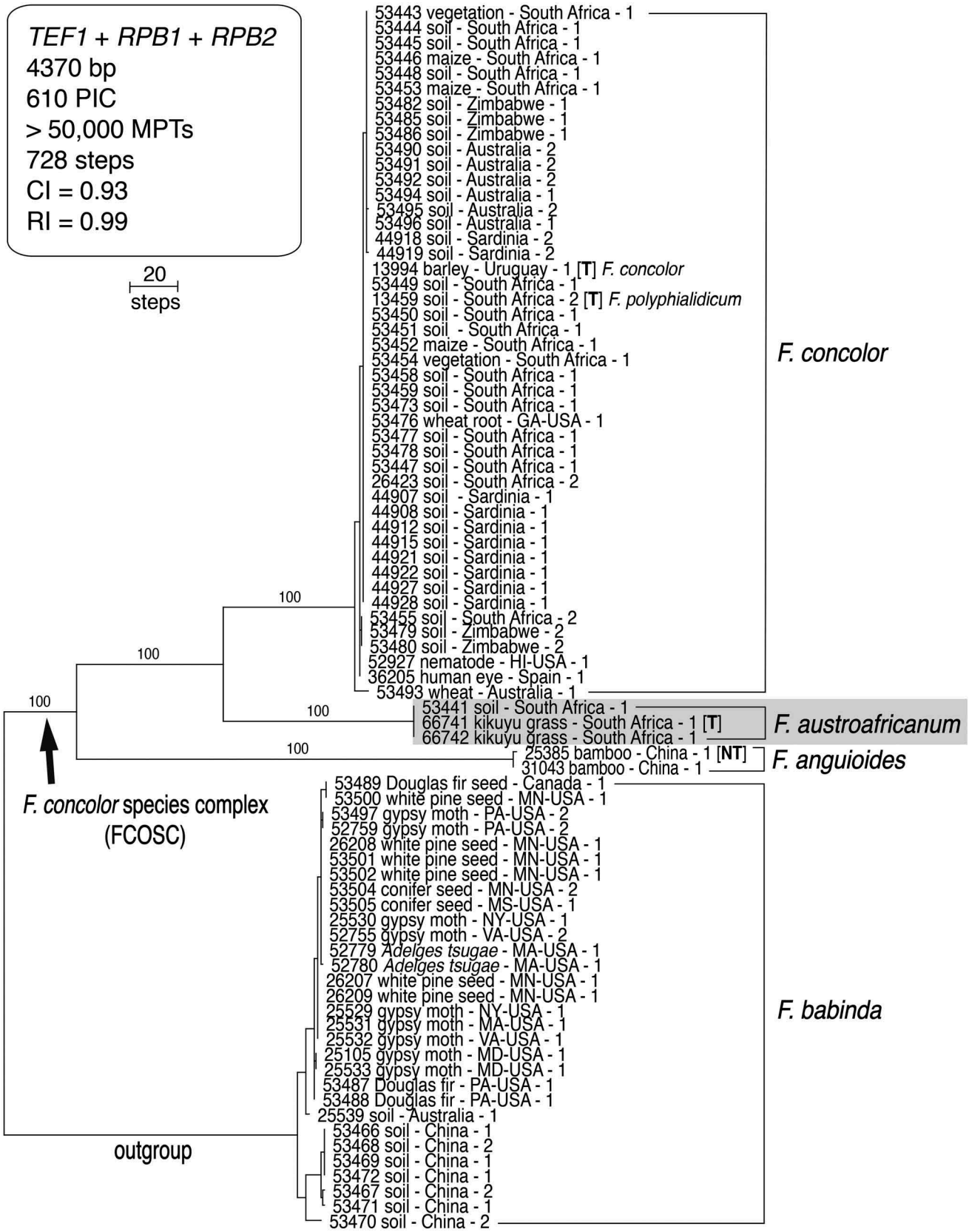

Figure 1. One of >50,000 most-parsimonious phylograms inferred from maximum parsimony (MP) analysis of a three-locus data set that included aligned partial sequences from *TEF1*, *RPB1*, and *RPB2*. The ingroup included representatives of three species in the *Fusarium concolor* species complex (FCOSC): *F. concolor* (N = 46), *F. austroafricanum* (N = 3, highlighted in gray), and *F. anguioides* (N =2), which were rooted on sequences of *F. babinda* based on more inclusive analyses (O'Donnell et al. 2013; Kim et al. 2017). Each strain was typed as *MAT1-1* (1) or *MAT1-2* (2) using PCR assays for *MAT* idiomorph (Kerényi et al. 2004; present study). CI = consistency index; MPTs = most-parsimonious trees; NT = neotype strain; PIC = parsimony-informative character; RI = retention index; T = type strain.

of *F. austroafricanum* from kikuyu grass were received as *F. redolens* (Botha et al. 2014), and the one from plant debris was previously reported as *F. polyphialidicum* (Marasas et al. 1986). Three quarters of the *F. concolor* isolates were received as *F. polyphialidicum*, including the ex-type strain from South Africa (NRRL 13459 = CBS 961.87). It shared the same three-locus haplotype as the ex-type strain of *F. concolor* from barley in Uruguay, together with NRRL 53476 from a wheat root in Georgia and several strains from Sardinian soil (FIG. 1). Most of the *F. concolor* isolates were recovered from soil or plant debris in soil (TABLE 1), but this species was also isolated from a nematode in Hawaii (NRRL 52927 = ARSEF 3042) and a human corneal ulcer in Spain (NRRL 36205 = CBS 111770). Thirty of the 31 strains that were identified molecularly as *F. babinda* were received as *F. polyphialidicum* or *Fusarium* sp. from diverse hosts/substrates and geographic origins (TABLE 1). Originally reported from wet sclerophyll and rainforests in eastern Australia and Tasmania (Summerell et al. 1995), results of the present study show that this species is associated with European gypsy moth (*Lymantria dispar*) and the Asian hemlock woolly adelgid (*Adelges tsugae*) in eastern United States, conifer seed in North America, and tea bush soil in China (TABLE 1).

Determination of mating type idiomorph and secondary metabolite biosynthetic potential.— Results of the Kerényi et al. (2004) PCR assay for *MAT* idiomorph revealed that strains of *F. concolor* were segregating for both idiomorphs in South Africa, Zimbabwe, Sardinia and Australia, and in isolates of *F. babinda* from gypsy moth larvae in the United States and Chinese soil. The three strains of *F. austroafricanum*, by way of contrast, were all typed as *MAT1-1*. BLASTn queries of the whole genome sequence data revealed that *F. austroafricanum* NRRL 53441, *F. anguioides* NRRL 25385, and *F. babinda* NRRL 25539 possessed a *MAT1-1* idiomorph, whereas *F. concolor* NRRL 13459 contained *MAT1-2*. Because the Kerényi et al. (2004) primers failed on *F. anguioides*, we used the whole genome sequence data to design a PCR assay for *MAT* idiomorph, which revealed that the two strains of *F. anguioides* from China were *MAT1-1*.

Genome sequences of *F. austroafricanum, F. concolor, F. anguioides*, and *F. babinda* were examined for the presence and absence of gene clusters that confer the ability to synthesize multiple *Fusarium* mycotoxins and pigments (TABLE 3). The only mycotoxin biosynthetic gene cluster that was present in all four species was the beauvericin/enniatin cluster. The fusaric acid and fusarin biosynthetic gene clusters were present in *F. babinda*, but these were absent in the other three species. Homologs of both culmorin biosynthetic genes were located on different contigs in *F. austroafricanum, F. concolor*, and *F. babinda*, suggesting that the two genes are not located in a gene cluster, but these are missing in *F. anguoides*. None of the species had a fumonisin, trichothecene, or zearalenone biosynthetic gene cluster. All four species had the biosynthetic gene clusters that confer the ability to synthesize carotenoid and fusarubin pigments (TABLE 3). The bikaverin biosynthetic gene cluster was only present in *F. babinda*, whereas the aurofusarin cluster was missing from all four species.

Twenty-two strains, representing the three species in the FCOSC, and the sister species *F. babinda*, were tested for their ability to produce mycotoxins and other biologically active metabolites on cracked maize cultures (SUPPLEMENTARY TABLE 1). None of the strains produced detectable levels of fumonisins (FB_1, FB_2, and FB_3), the depsipeptide mycotoxin beauvericin (BEA), and the mutagenic and carcinogenic mycotoxin fusarin C (FC). Moreover, of the four species analyzed,

Table 3. Analysis of mycotoxin and pigment biosynthetic gene clusters in genome sequences of members of the *F. concolor* (FCONSC) and *F. babinda* (FBASC) species complexes.

	FCONSC		FBASC	
Compound	*F. austroafricanum* NRRL 66741	*F. concolor* NRRL 13459	*F. anguoides* NRRL 25385	*F. babinda* NRRL 25539
Mycotoxins				
Beauvericin/enniatins	+	+	+	+
Culmorin	+	+	−	+
Fumonisins	−	−	−	−
Trichothecenes	−	−	−	−
Fusaric acid	−	−	−	+
Fusarin	−	−	−	+
Zearalenone	−	−	−	−
Pigments				
Aurofusarin	−	−	−	−
Bikaverin	−	−	−	+
Carotenoids	+	+	+	+
Fusarubin	+	+	+	+

Note. +, present; −, absent.

F. austroafricanum was the only one that failed to produce any of the 10 biologically active and toxic secondary metabolites we tested. The cytotoxic polyketide 8-*O*-methylbostrycoidin (MB), fusaric acid mycotoxin (FA), and red pigment bikaverin (BIK) were only detected in *F. babinda*, but in only 2–4 of the 10 strains tested. Detectable levels of the cyclic depsipeptide mycotoxin enniatin B (ENB) were produced by *F. anguioides* NRRL 25385 and 7/9 strains of *F. concolor*. Four strains of the latter species also produced low but detectable levels of the polar mycotoxin moniliformin (MON) (SUPPLEMENTARY TABLE 1).

Pathogenicity on spring wheat and mycotoxin quantification from wheat spikelets.—Of the eight isolates tested for pathogenicity on wheat (TABLE 4), *F. anguioides* NRRL 25385 and the three strains of *Fusarium austroafricanum* (NRRL 53441, 53489, 66741) were pathogenic and caused disease symptoms in the susceptible spring wheat cultivar Norm, but disease did not spread to the neighboring spikelets. *Fusarium babinda* NRRL 53497 and the two strains of *F. concolor* (NRRL 13459 and 13994) were nonpathogenic. Furthermore, none of the mycotoxins produced by these strains on cracked maize cultures were detected in the inoculated wheat spikelets. Only the positive-control strain, *F. graminearum* NRRL 29169 (Gz3639 = CBS 110271), was aggressive, spread to the neighboring spikelets, and caused bleaching of the entire wheat head 21 d post inoculation. Consistent with its ability to spread in the wheat head, NRRL 29169 *F. graminearum* was the only isolate that produced the virulence factor deoxynivalenol in planta (13 ± 8 µg deoxynivalenol/spikelet).

TAXONOMY

Fusarium austroafricanum A. Jacobs, I. Laraba & O'Donnell, sp. nov. FIGS. 1–3
MycoBank MB823959

Typification: SOUTH AFRICA. EASTERN CAPE: Humansdorp, a dried culture of PPRI 10408, originally isolated as an endophyte of *Pennisetum clandestinum* (kikuyu grass), Apr 2010, *A. Jacobs* (**holotype** PREM 62137). **Paratypes**: PREM 62138 (a dried culture of PPRI 23546 = NRRL 53441 = FRC M-2406 = DAOM 192987 = CBS 120990); PREM 62139 (a dried culture of PPRI 10412 = NRRL 66742). Ex-holotype cultures: PPRI 10408 = PPRI 23548 = NRRL 66741.

Etymology: austr + *africanum*, meaning from South Africa.

Colony color on PDA white to reddish white (7A2), reverse light orange (6A4). Aerial mycelium sparsely produced throughout colony. Colonies lacking distinct odor. Colony margin entire with optimal radial growth rate 3.3–3.5 mm/d at 30 C on PDA. Sclerotia and chlamydospores not observed on PDA; few chlamydospores produced on SNA but produced abundantly either singly or in intercalary or terminal clusters after 2 wk on SEA under alternating 12 h darkness/12 h fluorescent white and black light at 25 C, 9–20 µm in diam. Aerial conidiophores originating from substrate, unbranched or branched irregularly, dichotomously or sympodially, abundant toward center of colony, producing oval to obovoid 0-septate conidia accumulating in false heads on mostly subcylindrical mono- and polyphialides. Monophialides of aerial conidiophore: on SNA (8.5–)14.5–17(–21.5) × (2–)3.5–4.5(–6) µm in total range, 18.5 ± 1.02 × 4 ± 0.15 µm on average (± SD); on water agar (11.5–)15.5–20(–27.5) × (2.5–)3.5–4(–8) µm in total range, 18.5 ± 0.82 × 4 ± 0.21 µm on average (± SD). Polyphialides of aerial conidiophores: on SNA (7.5–)13–15.5(–26) × (2.5–)3–4.5(–6.5) µm in total range, 18.5 ± 0.95 × 4.5 ± 0.10 µm on average (± SD); on water agar (8–)15–22(–26) × (2–)3–3.5(–5.5) µm in total range, 18.5 ± 0.95 × 3 ± 0.11 µm on average (± SD). 0-Septate aerial conidia: on SNA (6.5–)9.5–11.5(–15.5) × (3–)4–5(–6.5) µm in total range, 10.5 ± 0.22 × 4.5 ± 0.10 µm on average (± SD); on water agar (5–)7–16.5(–25.5) × (4–)6–7.5(–9.5) µm in total range, 13 ± 0.78 × 6.5 ± 0.19 µm on

Table 4. Pathogenicity on wheat.

Species	NRRL no.[a]	Pathogenic[b]	Aggressive[c]
F. anguioides	25385	+	–
F. austroafricanum	53441	+	–
F. austroafricanum	53489	+	–
F. austroafricanum	66741	+	–
F. concolor	13994	–	–
F. concolor	13459	–	–
F. babinda	53497	–	–
F. graminearum	29169	+	+

[a]ARS Culture Collection, Peoria, Illinois.
[b]+, caused head blight symptoms; –, disease symptoms not discernible.
[c]+, isolate spread beyond the inoculated spikelet to neighboring spikelets; –, isolate did not spread beyond inoculated spikelet.

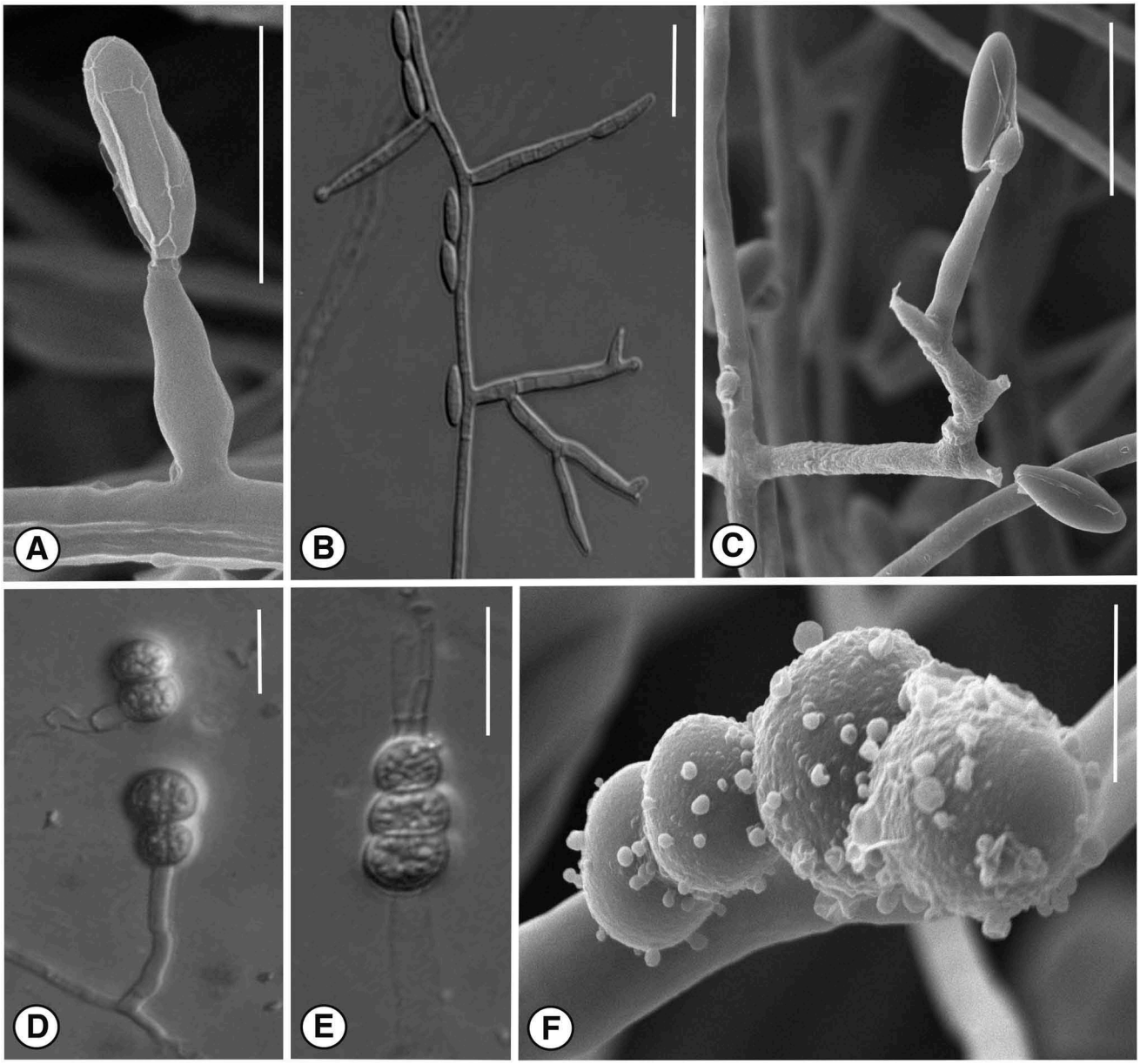

Figure 2. *Fusarium austroafricanum* NRRL 66741 (= PPRI 23548) cultured under a 12 h darkness/12 h fluorescent white and black light cycle at 25 C. A–C on SNA; D–F on SEA. A. Scanning electron micrograph (SEM) of monophialidic aerial conidiophore bearing 0-septate conidium. B. Differential interference contrast (DIC) light micrograph of substrate mycelium bearing monophialidic or mono- and polyphialidic conidiophores. C. SEM of sympodial branching, percurrently proliferating polyphialidic aerial conidiophore producing 0-septate oval to obovoid conidia. D–E. DIC micrographs of thick-walled catenate chlamydospores. F. SEM of terminal chain of chlamydospores with ornamented surface. Bars: A, C = 10 µm; B, D–E = 20 µm; F = 5 µm.

average (± SD). Sporodochial conidia cultured under alternating 12 h darkness/12 h fluorescent white and black light on SNA and water agar mostly produced on agar surface around filter paper falcate, apical cell blunt to slightly papillate, most 5-septate (i.e., 49.8% of 1000 counted) with slightly notched basal foot cell. Sporodochial conidiophores branched irregularly terminating in subcylindrical to subclavate monophialides (11–)12.5–15(–21) × (2.5–)3.5–4.5(–5) µm in total range, 14.5 ± 0.28 × 4 ± 0.11 µm. Sporodochia not observed on PDA. Sporodochial conidia 0–11-septate, but 95.9% 3–8-septate. Sporodochial conidia on SNA measuring: 3-septate: (25.5–)33–41(–50) × (4–)5–6(–7.5) µm in total range, 35.5 ± 0.86 × 5.5 ± 0.11 µm on average (± SD); 4-septate: (41–)46.5–53(–72) × (4.5–)5.5–7(–8) µm in total range, 50.5 ± 0.83 × 6 ± 0.13 µm on average (± SD); 5-septate: (45–)54–63(–77) × (4–)5–6(–7) µm in total range, 59 ± 1.03 × 5.5 ± 0.10 µm on average (± SD). Sporodochial conidia on water agar measuring: 4-septate: (29.5–)54.5–67(–80.5) ×

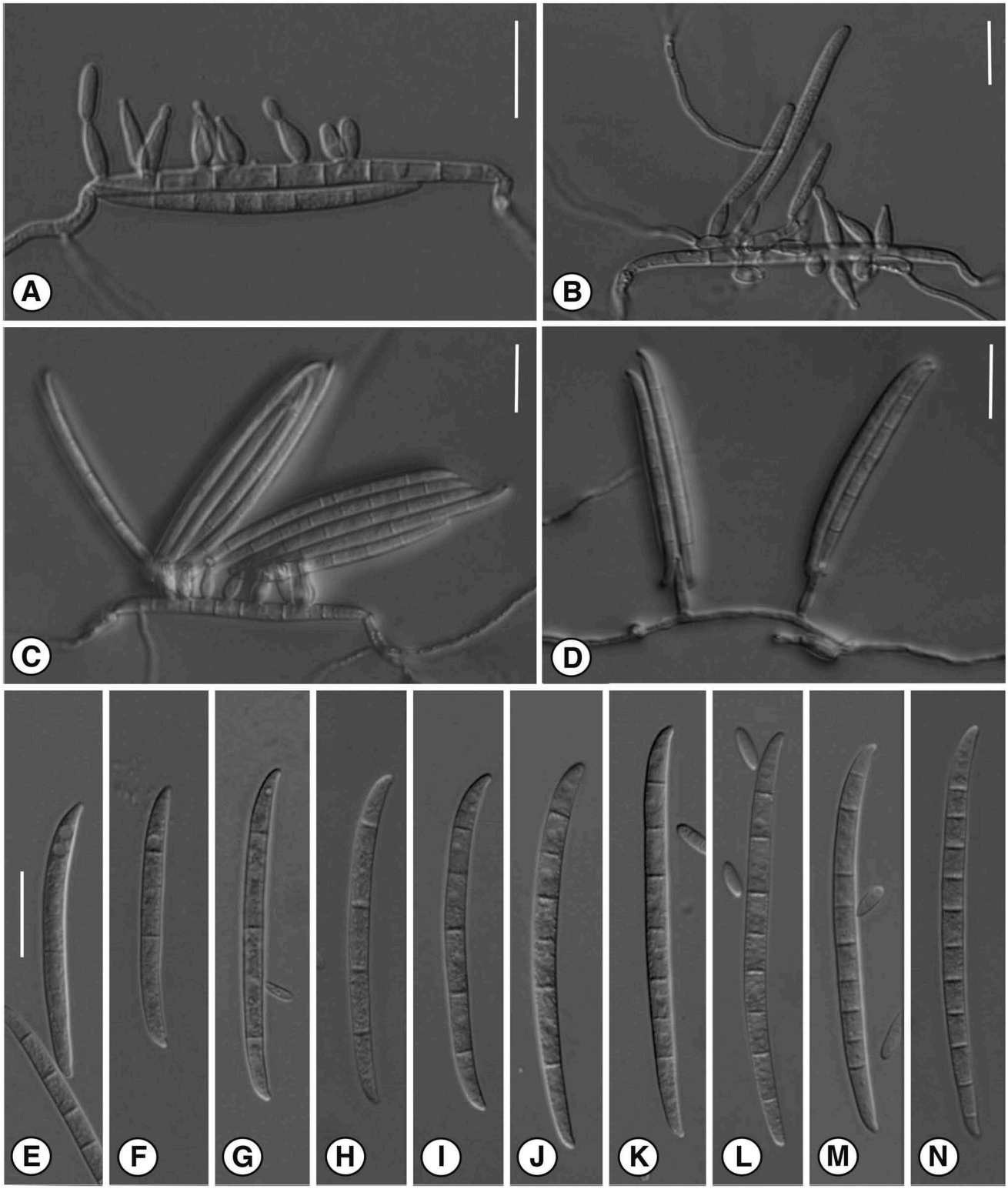

Figure 3. DIC micrographs of *Fusarium austroafricanum* NRRL 66741 (= PPRI 23548) cultured under an alternating 12 h darkness/12 h fluorescent white and black light cycle at 25 C on 2% water agar with filter paper. A–C. Microcycle conidiation. A–B. Monophialides producing conidia directly on multiseptate sporodochial conidia. C. Sporodochial conidium with monophialides and detached multiseptate conidia. D. Monophialides on substrate mycelium and detached multiseptate conidia. E–N. 1- to 11-septate sporodochial conidia. Bars: A–N = 20 µm.

(4.5–)5.5–6.5(–8) µm in total range, 61 ± 1.58 × 6 ± 0.13 µm on average (± SD); 5-septate: (44.5–)64.5–77.5 (–85) × (4–)5.5–7(–8) µm in total range, 70.5 ± 1.26 × 6 ± 0.12 µm on average (± SD); 6-septate: (57–)77–84 (–96) × (5–)6–7(–8) µm in total range, 81.5 ± 1.07 × 2.5 ± 0.12 µm on average (± SD); 7-septate: (74–)81.5–88 (–96) × (4.5–)6–6.5(–7.5) µm in total range, 85.5 ± 0.88 × 6.25 ± 1.02 µm on average (± SD); 8-septate: (76–) 88–92.5(–98.5) × (5–)5.5–6.5(–7.5) µm in total range, 95 ± 1.73 × 6 ± 0.20 µm on average (± SD).

Distribution: Humansdorp in Eastern Cape Province and Nelspruit in Mpumalanga Province, South Africa.

Additional strains examined: PPRI 10412 = NRRL 66742, ex kikuyu grass, Humansdorp, South Africa; PPRI 23546 = NRRL 53441 = FRC M-2406 = DAOM 192987 = CBS 120990, plant debris in soil, Mpumalanga, South Africa.

DISCUSSION

The three South African strains of *Fusarium austroafricanum* were resolved as a strongly supported genealogically exclusive lineage in the individual gene genealogies and the combined data set, thereby fulfilling the conservative operational criterion of genealogical concordance phylogenetic species recognition (GCPSR; Taylor et al. 2000; Dettman et al. 2003). This species is most similar morphologically to *F. concolor* and *F. babinda* (Reinking 1934; Marasas et al. 1986; Summerell et al. 1995); however, *F. austroafricanum* produces white to reddish white colonies on PDA, whereas those of *F. concolor* and *F. babinda* are white to pale orange and pale orange to violet, respectively. These three species can be distinguished by their morphologically distinct macroconidia. The apical macroconidial cell is blunt to slightly papillate in *F. austroafricanum*, strongly papillate in *F. concolor*, and slightly curved to hooked in *F. babinda*. Moreover, the basal macroconidial cell is slightly notched in *F. austroafricanum* compared with foot-shaped in *F. concolor* and *F. babinda*. *Fusarium austroafricanum* failed to produce sporodochia on CLA, whereas they were white to pale orange in the aerial mycelium or on carnation leaves in *F. concolor* (Marasas et al. 1986) and pale orange on carnation leaves in *F. babinda*.

Macroconidia were produced abundantly on water agar with filter paper from monophialides on macroconidia via a microcycle in the three strains of *F. austroafricanum*; however, microcycle conidiation was never observed in *F. concolor* and *F. babinda* grown under identical conditions. Microcycle conidiation has been reported in phylogenetically diverse fusaria, including putatively wild-type isolates of *F. culmorum* (Booth 1971), mutants of *Fusarium* sp. FSSC 11 (reported as *F. solani* f. sp. *pisi*) induced with *N*-methyl-*N*′-nitro-*N*-nitrosoguanidine (Kølmark 1984), and mutants of *F. verticillioides* and *F. graminearum* in which the global regulators of conidiogenesis, *veA* and *wetA*, respectively, were deleted (Li et al. 2006; Son et al. 2014). Given that *F. austroafricanum* only produced macroconidia via a microcycle on low-nutrient water agar, we speculate as posited for other fungi (Lapaire and Dunkle 2003; Jung et al. 2014) that the microcycle may allow this species to survive stressful environmental conditions. The three strains of *F. austroafricanum* from South Africa might be clones based on the absence of single-nucleotide polymorphisms (SNPs) in the three loci sequenced and results of the *MAT* PCR assay that revealed that all three strains are *MAT1-1*. The closely related species *F. concolor* and *F. babinda*, by comparison, are segregating for *MAT1-1* and *MAT1-2* idiomorphs locally on two continents, which suggests that further study might reveal that they possess a heterothallic sexual reproductive mode.

Results of the present study support the findings of Balmas et al. (2010) that *F. polyphialidicum* is a heterotypic synonym (taxonomic synonym) of *F. concolor* (Turland et al. 2018). Following its formal description based on a single culture from diseased barley near Montevideo, Uruguay (Reinking 1934), *F. concolor* was included in the taxonomic treatments of *Fusarium* by Wollenweber and Reinking (1935), Booth (1971), and Gerlach and Nirenberg (1982), and as *F. polyphialidicum* in Leslie and Summerell (2006), but not in Nelson et al. (1983). Reinking (1934) and Marasas et al. (1986) classified *F. concolor* in section *Arthrosporiella*, whereas Booth (1971) placed it in section *Gibbosum*, primarily because he failed to observe true microconidia in the deteriorated type culture CBS 183.34. However, because these and other sections are nonmonophyletic, the artificial morphology-based subgeneric sectional classification was replaced with reciprocally monophyletic clades referred to as species complexes (O'Donnell et al. 2013). The difficulty of using morphological data to identify these fusaria is reflected by our discovery that only 4/109 isolates analyzed in the present study were received correctly identified to species. BBA 63778 (= CBS 217.78 = NRRL 25483) ex *Pennisetum typhoideum* from Namibia, for example, was reported as *F. concolor* by Gerlach and Nirenberg (1982); however, this strain represents an undescribed species in the distantly related *F. chlamydosporum* species complex (TABLE 1).

Even though we discovered subtle phenotypic differences that can be used to distinguish *F. concolor*, *F. babinda*, and *F. austroafricanum*, we recommend sequencing a portion of *TEF1, RPB1*, or *RPB2* to obtain a definitive identification. This recommendation is

based on our discovery that only 1/46 *F. concolor* and 1/31 *F. babinda* strains were received identified correctly. In addition to its association with fruit rot of banana in Peninsular Malaysia (Murad et al. 2017), results of the present study confirm the presence of *F. concolor* in Australia (Gott et al. 1994) and extend its known distribution to North America where NRRL 53476 was recovered from a wheat root in Georgia. Two of the strains received as *F. polyphialidicum* were isolated from human mycotic infections. Our results confirm the identification of NRRL 36205 (= CBS 111770 = IHEM 19748) as *F. concolor* from a keratitis case in Spain (Guarro et al. 2003) but show that NRRL 25728 (= NRRL 25487 = CBS 463.91) from a human nail in Germany is a member of the *F. oxysporum* species complex, and not *F. concolor* as previously reported (O'Donnell et al. 2010). Like most other fusaria (Zhang et al. 2015), *F. concolor* NRRL 36205 from the corneal ulcer was broadly resistant to the eight antifungals tested by Triest et al. (2015).

Our discovery that 26 of the 31 strains received as *F. polyphialidicum* are *F. babinda* has advanced our knowledge of the geographic distribution and ecological associations of the latter species. Previously only known from wet schlerophyll and rain forests in eastern Australia and Tasmania, results of the present study together with data in GenBank show that *F. babinda* was recovered from tea bush soil and as an endophyte of conifer in China (GenBank DQ295144.1 as *F. polyphialidicum*), beech leaves in Belgium (GenBank KJ126259-KJ126260 as *F. polyphialidicum*; Triest et al. 2015), gypsy moth (*Lymantria dispar*) and Asian hemlock woolly adelgid (*Adelges tsugae*) in eastern United States (Hajek et al. 1993, 1997; reported as *Fusarium* sp. in O'Donnell et al. 2012), and conifer seeds in North America (as *F. polyphialidicum* in Ocamb et al. 2002). The discovery that *F. babinda* is associated with eastern white pine and Douglas fir in North America warrants further study to better understand the relationship and determine whether it is transmitted vertically in the seed.

Given that *F. concolor* was initially recovered from diseased barley (Reinking 1934), we conducted a pathogenicity experiment to assess whether members of the FCOSC and *F. babinda* could cause disease on wheat, a close relative of barley. Our data showed that *F. concolor* and *F. babinda* were not pathogenic on susceptible spring wheat cultivar Norm, whereas *F. anguioides* and *F. austroafricanum* were pathogenic but not aggressive as compared with the deoxynivalenol-producing *F. graminearum* NRRL 29169 strain, which spread throughout the spike (Goswami and Kistler 2004). Results of the present study highlight the importance of verifying the identity of strains molecularly that are tested for mycotoxin production. For example, in prior studies, *F. concolor* was incorrectly reported to produce fumonisin FB_1 (Abbas and Ocamb 1995), diacetoxyscirpenol trichothecene (Shi et al. 2017), and moniliformin (Rabie et al. 1982) mycotoxins. Lineages of fumonisin and trichothecene toxin–producing fusaria, however, are distantly related to the FCOSC (O'Donnell et al. 2013; Kim et al. 2017); none of these fusaria produced fumonisins and trichothecene toxins on cracked maize cultures in the present study (SUPPLEMENTARY TABLE 1), and the biosynthetic gene clusters that are required for their production were not detected in their genomes (Kim et al. 2017). To our knowledge, the present study is the first valid report that some strains of *F. concolor* can produce moniliformin and enniatin B toxins in vitro; also, the latter toxin was detected for the first time in *F. anguioides*. The one published report that *F. concolor* can produce moniliformin (Rabie et al. 1982) is inaccurate because the strain they studied (= BBA 63778 = NRRL 25483 = CBS 217.78) is a distantly species that is nested in the *F. chlamydosporum* species complex. Our discovery that only 4/9 *F. concolor* strains tested produced moniliformin toxin, albeit it at low levels, coupled with the failure to detect this toxin in authentic strains of this species (Chelkowski et al. 1990; Schütt 2001), emphasizes the importance of not over generalizing that a species is a nonproducer based on analyses of a small number of strains. Ongoing research focused on identifying the genes essential for moniliformin production should facilitate development of molecular tools to elucidate the phylogenetic diversity of fusaria with the potential to produce this toxin (Proctor, pers. commun.). Consistent with the findings of Schütt (2001), moniliformin toxin was not detected in the 10 strains of *F. babinda* we tested; however, several strains of this species produced the broad-spectrum phytotoxin fusaric acid (5-butylpicolinic acid), the red naphthoquinone pigment bikaverin, and the cytotoxin 8-*O*-methylbostrycoidin (Busman 2017). As originally reported for *F. verticillioides* (Brown et al. 2012) and *F. fujikuroi* (Wiemann et al. 2009), the genes responsible for fusaric acid and bikaverin biosynthesis, respectively, are clustered in *F. babinda*. The three strains of *F. austroafricanum* were unique among the four species tested in that none of the 10 mycotoxins and pigments that we assayed for were detected in cracked maize kernel cultures. However, gene clusters responsible for synthesis of two of the metabolites (bostrycoidins and enniatins) were present in *F. austroafricanum*, and based on their sequences, the genes in the clusters appear to be functional. Therefore, this species may

be able to produce bostrycoidins and enniatins under conditions other than those examined in the current study. Given the ability of this species to grow endophytically in kikuyu grass, and our discovery of intact beauvericin, enniatin, fusarubin, and bostrycoidin gene clusters in their whole genomes, strains of this species should be tested for their ability to produce these toxins in planta to further assess whether they might have contributed to the outbreaks of kikuyu poisoning of dairy cows in South Africa. Assuming the outbreaks were due to a mycotoxicosis, accurate identification of the species and the toxins produced in planta would represent an important step toward prevention and control.

ACKNOWLEDGMENTS

The authors would like to thank Dr. Shaun Pennycook for his valuable assistance with the Latin binomial. The authors also thank Gail Doehring, Amy McGovern, Nathane Orwig, Deborah S. Shane, Jennifer Teresi, and Arthur Thompson for skilled assistance in various aspects of this study.

Disclaimer: Mention of trade names or commercial products in this publication is solely for the purpose of providing specific information and does not imply recommendation or endorsement by the US Department of Agriculture (USDA). USDA is an equal opportunity provider and employer.

ORCID

Imane Laraba http://orcid.org/0000-0002-2118-8773
Mark Busman http://orcid.org/0000-0001-9750-064X
Robert H. Proctor http://orcid.org/0000-0001-5400-1680
Susan P. McCormick http://orcid.org/0000-0002-7824-6372
Kerry O'Donnell http://orcid.org/0000-0001-6507-691X

LITERATURE CITED

Abbas HK, Ocamb CM. 1995. First report of production of fumonisin B1 by *Fusarium polyphialidicum* collected from seeds of *Pinus strobus*. Plant Disease 79:642.

Aoki T, O'Donnell K, Geiser DM. 2014. Systematics of key phytopathogenic *Fusarium* species: current status and future challenges. Journal of General Plant Pathology 80:189–201.

Aoki T, Vaughan MM, McCormick SP, Busman M, Ward TJ, Kelly A, O'Donnell, K, Johnston PR, Geiser DM. 2015. *Fusarium dactylidis* sp. nov., a novel nivalenol toxin-producing species sister to *F. pseudograminearum* isolated from orchard grass (*Dactylis glomerata*) in Oregon and New Zealand. Mycologia 107:409–418.

Balmas V, Migheli Q, Scherm B, Garau P, O'Donnell K, Ceccherelli G, Kang S, Geiser DM. 2010. Multilocus phylogenetics show high levels of endemic fusaria inhabiting Sardinian soils (Tyrrhenian Islands). Mycologia 102:803–812.

Booth C. 1971. The genus *Fusarium*. Kew, UK: Commonwealth Mycological Institute. 237 p.

Botha CJ, Truter M, Jacobs A. 2014. *Fusarium* species isolated from *Pennisetum clandestinum* collected during outbreaks of kikuyu poisoning in cattle in South Africa. Onderstepoort Journal of Veterinary Research 81:1–8.

Brown DW, Butchko RAE, Busman M, Proctor RH. 2012. Identification of gene clusters associated with fusaric acid, fusarin, and perithecial pigment production in *Fusarium verticillioides*. Fungal Genetics and Biology 49:521–532.

Brown DW, Lee S-H, Kim L-H, Ryu J-G, Lee S, Seo Y, Kim YH, Busman M, Yun S-H, Proctor RH, Lee T. 2015. Identification of a 12-gene fusaric acid biosynthetic gene cluster in *Fusarium* species through comparative and functional genomics. Molecular Plant-Microbe Interactions 28:319–332.

Busman M. 2017. Utilization of high performance liquid chromatography coupled to tandem mass spectrometry for characterization of 8-*O*- methylbostrycoidin production by species of the fungus *Fusarium*. Journal of Fungi 3:43.

Busman M, Butchko RA, Proctor RH. 2012. LC-MS/MS method for the determination of the fungal pigment bikaverin in maize kernels as an indicator of ear rot. Food Additives & Contaminants: Part A 29:1736–1742.

Chelkowski J, Zawadzki M, Zaikowski P, Logrieco A, Bottalico A. 1990. Moniliformin production by *Fusarium* species. Mycotoxin Research 6:41–45.

Dettman JR, Jacobson DJ, Taylor JW. 2003. A multilocus genealogical approach to phylogenetic species recognition in the model eukaryote *Neurospora*. Evolution 57:2703–2720.

Edgar RC. 2004. MUSCLE: multiple sequence alignment with high accuracy and high throughput. Nucleic Acids Research 32:1792–1797.

Edwards J, Auer D, de Alwis S-K, Summerell B, Aoki T, Proctor RH, Busman M, O'Donnell K. 2016. *Fusarium agapanthi* sp. nov., a novel bikaverin and fusarubin-producing leaf and stem spot pathogen of *Agapanthus praecos* (African lily) from Australia and Italy. Mycologia 108:981–992.

Fisher NL, Burgess LW, Toussoun TA, Nelson PE. 1982. Carnation leaves as a substrate and for preserving cultures of *Fusarium* species. Phytopathology 72:151–153.

Gerlach W, Nirenberg HI. 1982. The genus *Fusarium*—a pictorial atlas. Mitteilungen aus der Biologischen Bundesanstalt für Land- und Forstwirtschaft Berlin-Dahlem 209:1–406.

Goswami RS, Kistler HC. 2004. Heading for disaster: *Fusarium graminearum* on cereal crops. Molecular Plant Pathology 5:515–525.

Gott KP, Burgess LW, Balmas V, Duff J. 1994. Mycogeography of *Fusarium: Fusarium* species in soils from Palm Valley, central Australia. Australasian Plant Pathology 23:112–117.

Gräfenhan T, Johnston PR, Vaughan MM, McCormick SP, Proctor RH, Busman M, Ward TJ, O'Donnell K. 2016. *Fusarium praegraminearum* sp. nov., a novel nivalenol mycotoxin-producing pathogen from New Zealand can induce head blight on wheat. Mycologia 108:1229–1239.

Guarro J, Rubio C, Gené J, Cano J, Gil J, Benito R, Moranderia MJ, Miguez E. 2003. Case of keratitis caused by an uncommon *Fusarium* species. Journal of Clinical Microbiology 41:5823–5826.

Hajek AE, Elkinton JS, Humber RA. 1997. Entomopathogenic hyphomycetes associated with gypsy moth larvae. Mycologia 89:825–829.

Hajek AE, Nelson PE, Humber RA, Perry JL. 1993. Two *Fusarium* species pathogenic to gypsy moth, *Lymantria dispar*. Mycologia 85:937–940.

Herron DA, Wingfield MJ, Wingfield BD, Rodas CA, Marincowitz S, Steenkamp ET. 2015. Novel taxa in the *Fusarium fujikuroi* species complex from *Pinus* spp. Studies in Mycology 80:131–150.

Jung B, Kim S, Lee J. 2014. Microcycle conidiation in filamentous fungi. Mycobiology 42:1–5.

Kerényi Z, Moretti A, Waalwijk C, Oláh B, Hornok L. 2004. Mating type sequences in asexually reproducing *Fusarium* species. Applied and Environmental Microbiology 70:4419–4423.

Kim H-S, Proctor RH, Brown D. 2017. Comparative genomic analysis of secondary metabolite gene clusters in 207 isolates of *Fusarium*. In: 29th Fungal Genetics Conference; Pacific Grove, California; March 14–19. Rockville, Maryland: The Genetics Society of America. p. 170, Abstract 297F.

Klotz LV, Nelson PE, Toussoun TA. 1988. A medium for enhancement of chlamydospore formation in *Fusarium* species. Mycologia 80:108–109.

Kølmark HG. 1984. Mutants with continuous microcycle conidiation in the filamentous fungus *Fusarium solani* f. sp. *pisi*. Molecular and General Genetics 198:12–18.

Kornerup A, Wanscher JH. 1978. Methuen handbook of color. 3rd ed. London: Methuen. 252 p.

Lapaire CL, Dunkle LD. 2003. Microcycle conidiation in *Cercospora zeae-maydis*. Phytopathology 93:193–199.

Laraba I, Keddad A, Boureghda H, Abdallah N, Vaughan MM, Proctor RH, Busman M, O'Donnell K. 2018. *Fusarium algeriense*, sp. nov., a novel toxigenic crown rot pathogen of durum wheat from Algeria is nested in the *Fusarium burgessii* species complex. Mycologia 109:935–950.

Laurence MH, Summerell BA, Burgess LW, Liew ECY. 2011. *Fusarium burgessii* sp. nov. representing a novel lineage in the genus *Fusarium*. Fungal Diversity 49:101–112.

Leslie JF, Summerell BA. 2006. The *Fusarium* laboratory manual. Ames, Iowa: Blackwell Professional Publishing. 388 p.

Li S, Myung K, Guse D, Donkin B, Proctor RH, Grayburn WS, Calvo AM. 2006. *FvVE1* regulates filamentous growth, the ratio of microconidia to macroconidia and cell wall formation in *Fusarium verticillioides*. Molecular Microbiology 62:1418–1432.

Marasas WFO, Nelson PE, Toussoun TA. 1986. *Fusarium polyphialidicum*, a new species from South Africa. Mycologia 78:678–682.

Munkvold GP. 2017. *Fusarium* species and their associated mycotoxins. In: Moretti A, Susca A, eds. Mycotoxigenic fungi: methods and protocols. New York: Humana Press. p. 51–106.

Murad NBA, Nor NMIM, Shohaimi S, Zainudin NAIM. 2017. Genetic diversity and pathogenicity of *Fusarium* species associated with fruit rot disease in banana across Peninsular Malaysia. Journal of Applied Microbiology 123:1533–1546.

Nelson PE, Toussoun TA, Marasas WFO. 1983. *Fusarium* species: an illustrated manual for identification. University Park, Pennsylvania: The Pennsylvania State University Press. 193 p.

Nelson PE, Toussoun TA, Marasas WFO. 1995. Neotypification and emended description of *Fusarium anguioides*. Mycologia 87:543–546.

Nirenberg HI. 1976. Untersuchungen über die morphologische und biologische. Differenzierung in der *Fusarium*-Sektion *Liseola*. Mitteilungen aus der Biologischen Bundesanstalt für Land- und Forstwirtschaft Berlin-Dahlem 169:1–117.

Nirenberg HI, O'Donnell K. 1998. New *Fusarium* species and combinations within the *Gibberella fujikuroi* species complex. Mycologia 90:434–458.

O'Donnell K, Cigelnik E, Nirenberg HI. 1998. Molecular systematics and phylogeography of the *Gibberella fujikuroi* species complex. Mycologia 90:465–493.

O'Donnell K, Humber RA, Geiser DM, Kang S, Park B, Robert VARG, Crous PW, Johnston PR, Aoki T, Rooney AP, Rehner SA. 2012. Phylogenetic diversity of insecticolous fusaria inferred from multilocus DNA sequence data and their molecular identification via FUSARIUM-ID and *Fusarium MLST*. Mycologia 104:427–445.

O'Donnell K, Rooney AP, Proctor RH, Brown DW, McCormick SP, Ward TJ, Frandsen RJN, Lysøe E, Rehner SA, Aoki T, Robert VARG, Crous PW, Groenewald JZ, Kang S, Geiser DM. 2013. Phylogenetic analyses of *RPB1* and *RPB2* support a middle Cretaceous origin for a clade comprising all agriculturally and medically important fusaria. Fungal Genetics and Biology 52:20–31.

O'Donnell K, Sutton DA, Fothergill A, McCarthy D, Rinaldi MG, Brandt ME, Zhang N, Geiser DM. 2008. Molecular phylogenetic diversity, multilocus haplotype nomenclature, and in vitro antifungal resistance within the Fusarium solani species complex. Journal of Clinical Microbiology 46:2477–2490.

O'Donnell K, Sutton DA, Rinaldi MG, Gueidan C, Crous PW, Geiser DM. 2009. Novel multilocus sequence typing scheme reveals high genetic diversity of human pathogenic members of the Fusarium incarnatum-F. equiseti and F. chlamydosporum species complexes within the United States. Journal of Clinical Microbiology 47:3851–3861.

O'Donnell K, Sutton DA, Rinaldi MG, Sarver BAJ, Balajee SA, Schroers H-J, Summerbell RC, Robert VARG, Crous PW, Zhang N, Aoki T, Jung K, Park J, Lee Y-H, Kang S, Park B, Geiser DM. 2010. Internet-accessible DNA sequence database for identifying fusaria from human and animal infections. Journal of Clinical Microbiology 48:3708–3718.

Ocamb CM, Juzwik J, Martin FB. 2002. *Fusarium* spp. and *Pinus strobus* seedlings: root disease pathogens and taxa associated with seed. New Forests 24:67–79.

Rabie CJ, Marasas WFO, Thiel PG, Lübben A, Vleggaar R. 1982. Moniliformin production and toxicity of different *Fusarium* species from southern Africa. Applied and Environmental Microbiology 43:517–521.

Reinking OA. 1934. Interesting new Fusaria. Zentralblatt für Bakteriologie und Parasitenkunde Abteilung 2. 89:509–514.

Sandoval-Denis M, Guarnaccia V, Polizzi G, Crous PW. 2018. Symptomatic *Citrus* trees reveal a new pathogenic

lineage in *Fusarium* and two new *Neocosmospora* species. Persoonia 40:1–15.

Schütt F. 2001. Moniliforminbildung von *Fusarium*-Arten unter definierten Bedingungen [PhD dissertation]. Berlin, Germany: Technischen Universität Berlin. 173 p.

Sherbakoff CD. 1915. Fusaria on potatoes. Memoirs of Cornell University Agricultural Experiment Station 6:87–270.

Shi W, Tan Y, Wang S, Gardiner DM, De Saeger S, Liao Y, Wang C, Fan Y, Wang Z, Wu A. 2017. Mycotoxigenic potentials of *Fusarium* species in various culture matrices revealed by mycotoxin profiling. Toxins 9:6.

Son H, Kim M-G, Min K, Lim JY, Choi GJ, Kim J-C, Chae S-K, Lee Y-W. 2014. *WetA* is required for conidiogenesis and conidium maturation in the ascomycete fungus *Fusarium graminearum*. Eukaryotic Cell 13:87–98.

Stevens RR. 1974. Mycology guidebook. Seattle, Washington: University of Washington Press. 703 p.

Summerell BA, Rugg CA, Burgess LW. 1995. Characterization of *Fusarium babinda* sp. nov. Mycological Research 99:1345–1348.

Swofford DL. 2003. PAUP*. Phylogenetic Analysis Using Parsimony (and other methods), Version 4.0b10. Sunderland, Massachusetts: Sinauer Associates.

Taylor JW, Jacobson DJ, Kroken S, Kasuga T, Geiser DM, Hibbett DS, Fisher MC. 2000. Phylogenetic species recognition and species concepts in fungi. Fungal Genetics and Biology 31:21–32.

Triest D, Stubbe D, De Cremer K, Piérard D, Normand A-C, Piarroux R, Detandt M, Hendricks M. 2015. Use of matrix-assisted laser desorption ionization–time of flight mass spectrometry for identification of molds of the *Fusarium* genus. Journal of Clinical Microbiology 53:465–476.

Turland NJ, Wiersema JH, Barrie FR, Greuter W, Hawksworth DL, Herendeen PS, Knapp S, Kusber W-H, Li D-Z, Marhold K, May TW, McNeill J, Monro AM, Prado J, Price MJ, Smith GF. eds. 2018. International Code of Nomenclature for algae, fungi, and plants (Shenzhen Code) adopted by the Nineteenth International Botanical Congress Shenzhen, China, July 2017. Regnum Vegetabile 159. Glashütten, Germany: Koeltz Botanical Books. 254 p.

Uhlig S, Petersen D, Flåøyen A, Wilkins A. 2005. 2-Amino-14,16-dimethyloctadecan-3-ol, a new sphingosine analogue toxin in the fungal genus *Fusarium*. Toxicon 46:513–522.

Wiemann P, Willmann A, Straeten M, Kleigrewe K, Beyer M, Humpf HU, Tudzynski B. 2009. Biosynthesis of the red pigment bikaverin in *Fusarium fujikuroi*: genes, their function and regulation. Molecular Microbiology 72:931–946.

Wollenweber HW, Reinking OR. 1935. Die Fusarien, iher Beschreibung, Schadwirkung und Bekämpfung. Berlin, Germany: Paul Parey. 355 p.

Zhang SX, O'Donnell K, Sutton DA. 2015. *Fusarium* and other opportunistic hyaline fungi. In: Jorgensen JH, Pfaller MA, Carroll KC, Funke G, Landry ML, Richter SS, Warnock DW, eds. Manual of clinical microbiology. Washington, DC: ASM Press. p. 2057–2086.

Zhou X, O'Donnell K, Aoki T, Smith JA, Kasson MT, Cao Z-M. 2016. Two novel *Fusarium* species that cause canker disease of prickly ash (*Zanthoxylum bungeanum*) in northern China form a novel clade with *Fusarium torreyae*. Mycologia 108:668–681.

Zwickl DJ. 2006. Genetic algorithm approaches for the phylogenetic analysis of large biological sequence data sets under the maximum likelihood criterion. GARLI 2.01. [cited 2017 Dec]. Available from: https://www.phylo.org/